ON HAMMERSHOCK PROPAGATION IN A SUPERSONIC FLOW FIELD

A. Robert Porro
National Aeronautics and Space Administration, Glenn Research Center
Cleveland, OH 44135, USA

Keywords: *Supersonic Inlets, Inlet Unstart*

Abstract

A wind tunnel test program was conducted to acquire flow-field data during a supersonic propulsion system compressor stall and inlet unstart sequence. The propulsion system consisted of a mixed-compression, two-dimensional bifurcated inlet coupled to a General Electric J85-13 turbojet engine. The propulsion system was mounted beneath a large flat plate that simulated an underwing propulsion pod installation. Transient flow-field pitot pressure and wing simulator surface static pressure data were acquired during multiple compressor stall and inlet unstart events at a free-stream Mach number of 2.20.

The experimental results obtained in this investigation indicate that a supersonic propulsion system compressor stall-inlet unstart transient event adversely affects the surrounding local flow field. The data show that the stall-unstart event affects the surrounding flow field on a millisecond time scale and causes a three-dimensional expanding wave front called a hammershock to propagate outward from the inlet. The flow nearest the wing simulator separates from the surface during the transient event. At the end of the transient event, a distinct process occurs wherein the affected flow field recovers to free-stream conditions and the wing simulator boundary layer reattaches to the flow surface.

1 Introduction

Inlet systems for aircraft gas turbine propulsion systems can experience a high pressure transient when a compressor stall occurs. The pressure transient is an overpressure due to the formation of a compression wave at the engine face and is commonly called a hammershock. If the overpressure is severe enough, this compression wave propagates upstream through the propulsion system inlet flowpath into the surrounding flow field. In the case of a supersonic propulsion system that uses a mixed compression inlet, the propagating compression wave destabilizes the established shock wave structure and causes the inlet to unstart.

This hammershock propagation phenomenon can have a detrimental effect on the aircraft and can cause stability and control problems leading to a catastrophic accident. In extreme cases, the hammershock propagation into the flow field induces sufficient local flow field distortion to stall an adjacent propulsion system. An experimental study was conducted at NASA Glenn Research Center to investigate the characteristics of hammershock disturbance propagation into the flow field surrounding a supersonic propulsion system due to engine compressor stall and subsequent inlet unstart.

The objective of this test program was to assess the underwing flow field of a propulsion system during an engine compressor stall and subsequent inlet unstart. The experimental research testing was conducted in the NASA Glenn 10- by 10- Foot Supersonic Wind Tunnel (SWT). The representative propulsion pod consisted of a two-dimensional-bifurcated inlet mated to an operating turbojet engine. The propulsion pod was mounted below a large flat plate that acted as a wing simulator to allow realistic boundary layers to form at the inlet cowl plane. Because the entire stall-unstart-hammershock event occurred on the order of 40

ms, unique transient flow-field instrumentation was developed for this program. Transient flow field and wing simulator surface static pressure data were acquired during multiple stall/unstart sequences using moveable instrumentation strut platforms. The results reported herein documents the observed flow physics of the transient hammershock propagation phenomenon.

2 Symbols

L_c	characteristic model length, 16 in.
M	Mach number
P	pressure, psia
Re	Reynolds number
T	temperature, R
t	time, s
X	axial distance relative to inlet cowl plane, in.
Y	spanwise (lateral) distance relative to propulsion system centerline, in.
Z	Distance below wing simulator (perpendicular to wing simulator surface), in.

Subscripts:

o	free stream (total) condition
t	pitot pressure
s	static pressure

3 Experimental Approach

3.1 Facility

The experimental testing was conducted in the 10- by 10-Foot Supersonic Wind Tunnel at Glenn Research Center. Details of the facility and its operation can be found in reference 1. This continuous-flow wind tunnel has a Mach number range of 2.0 to 3.5 and can operate in two cycle modes, aerodynamic and propulsion. The aerodynamic cycle is a closed-loop multipass mode similar to the operation of other large wind tunnels. The propulsion cycle is an open-loop, one-pass mode of operation unique to the 10- by 10-Foot Supersonic Wind Tunnel. In this cycle, freshly-conditioned ambient atmospheric air enters the circuit upstream of the test section through the air dryer, accelerates to supersonic speeds through the converging-diverging nozzle, enters the test section, and exits the tunnel circuit downstream through the muffler. Because a running turbojet engine was used in this investigation, the facility was operated in the propulsion cycle mode to avoid recirculating air contaminated by products of combustion throughout the facility.

3.2 Experimental Hardware

A photograph of the wind tunnel test hardware installation in the 10- by 10-Foot SWT is shown in figure 1. The main hardware components were (1) a wing simulator plate, (2) a mixed compression, two-dimensional-bifurcated supersonic inlet, (3) a General Electric (GE) J85-13 turbojet engine, and (4) instrumentation struts.

The wing simulator and inlet-engine combination simulated an underwing propulsion system installation. The inlet cowl lip leading edge was located outside of the wing simulator boundary layer to avoid boundary layer ingestion in the inlet during steady-state operating conditions. The instrumentation struts were used to acquire the flow-field data and were mounted to the wing simulator. The design and placement of the instrumentation struts minimized the interference with the free-stream flow field in the vicinity of the propulsion system.

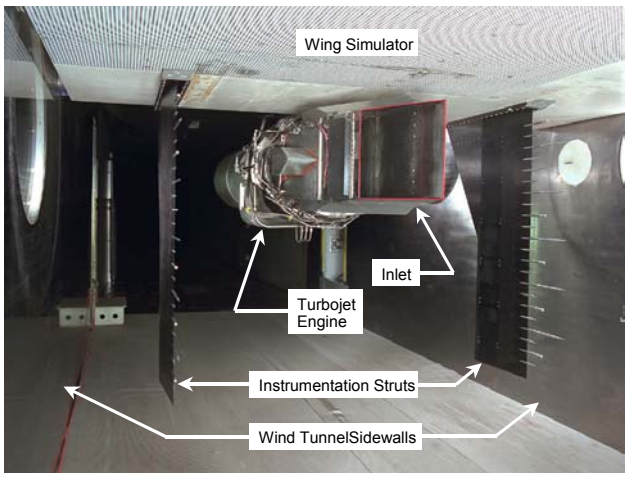

Fig. 1. Experimental hardware installation in 10- by 10- Foot Supersonic Wind Tunnel.

3.2.1 Inlet model

The inlet model is a mixed-compression, two-dimensional bifurcated flow-path design. The bifurcated design results in two identical flow passages that split the incoming flow around the inlet vertical centerline so that they eventually merge in the subsonic diffuser portion of the inlet.

The inlet model also had a bypass flow system to provide inlet-engine mass flow matching and emergency full-mass-flow overboard bypass in the event of an engine rotor lockup. The bypass flow system consisted of a cavity in the subsonic diffuser with four external doors to control the overboard bypass flow rate.

3.2.2 Turbojet engine

The engine portion of the propulsion system used in this investigation was a modified GE J85-13 turbojet engine with afterburner assembly installed. The first stage turbine nozzle area was reduced by 14 percent relative to the nominal J85-13 engine, which was done primarily to avoid turbine overtemperature during the compressor stall sequence. This modification allowed the engine compressor to operate at a higher pressure ratio for a given turbine inlet temperature.

The afterburner assembly was used only to induce engine compressor stall by actuation of the variable-area exit nozzle (VEN); the thrust-producing components were not active. To facilitate controlled engine compressor stalls, blockage plates were installed on the leaves of the VEN to provide additional exit area reduction.

3.2.3 Wing simulator

A large flat plate, nominally 10 ft wide by 18 ft long, was installed in the 10- by 10-Foot SWT to serve as a wing simulator. The long axial length allowed thick turbulent boundary layers to form toward the trailing edge of the plate where the inlet model was positioned beneath the flow surface. A view of the wing simulator installation in the wind tunnel is shown in figure 2.

The wing simulator was instrumented with an array of surface static pressure taps in the vicinity of the propulsion system. Figure 3 depicts the wing simulator nominal static tap locations in the static pressure array used for the results presented in this report. The axial row near the spanwise centerline is offset from the true model centerline at $Y/L_c = 0.08$. Since the objective of this test program was to acquire data during a transient unstart event, an array of 37 high-response dynamic pressure transducers were used to monitor the transient surface static pressure.

Fig. 2. Wing simulator installation in 10- by 10-Foot Supersonic Wind Tunnel.

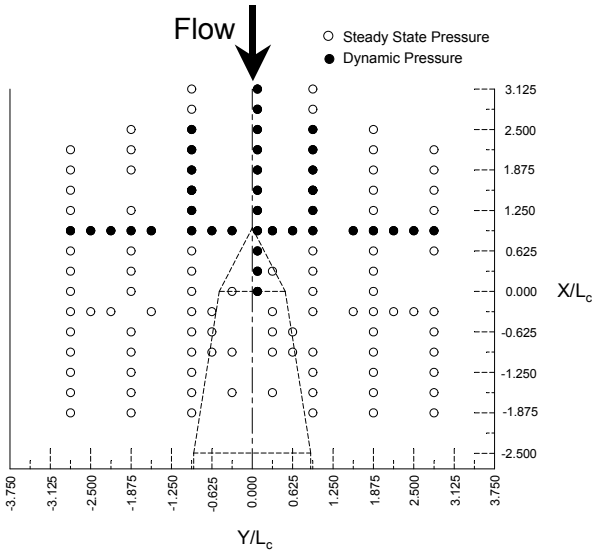

Fig. 3. Wing simulator nominal static tap locations (view from above).

3.2.4 Flow-field instrumentation

The bulk of the transient flow-field data were acquired by high-response pressure probes

mounted on instrumentation strut platforms. Details of the probe designs are given in reference 2. The 60-in.-long struts offers the ability to instrument a significant portion of the flow field in the vicinity of the propulsion system. The leading edge of each strut is a 10^{o} included angle that insures the shock emanating from the strut leading edge does not interfere with the flow field of interest in the vicinity of the propulsion system.

3.3 Experimental Technique

The objective of the test program was to acquire detailed flow-field data in the vicinity of a supersonic propulsion system during a transient engine compressor stall-inlet unstart sequence. To accomplish this goal, an effective integrated inlet and engine control system was developed and implemented. Effective stall-unstart procedures and an efficient flow-field data acquisition strategy were developed, and the type of stall-unstart events to be investigated was chosen.

3.3.1 Inlet-engine control system

The integrated inlet-engine control system developed for this investigation operated all the inlet variable geometry and engine parameters to match performance under the required operating conditions. Under normal operations, the inlet controls manipulated each ramp and pair of bypass doors on each side of the bifurcated inlet. In the event of an inlet unstart, an override control took over the normal operating control to stabilize and restart the inlet.

The inlet-engine control system was operated in the automatic shock control mode. In this mode, the controller positioned the terminal shock in the inlet to set the inlet total pressure recovery by manipulating the overboard mass-flow bypass doors located in the subsonic diffuser. The control feedback signal, the ratio of throat static pressure to free-stream total pressure, served in place of a direct shock position sensor feedback. Set point values for this pressure ratio were determined from previous performance tests.

Operation of the engine was accomplished through a graphical operator interface networked to a digital control system. The engine control system was integrated with the inlet controls and servosystems on the engine. The variable exit nozzle (VEN) could be moved manually or left on schedule to move automatically. The engine controls also included an option to remove the VEN from the automatic operation schedule and ramp it closed at a variable rate. This automated ramp function caused the engine compressor to stall by reducing the exit area of the afterburner nozzle while maintaining the corrected speed. Accurately maintaining engine speed during the VEN closure was critical for the unstart phenomenon to be captured at the correct operating point.

3.3.2 Stall-unstart procedures

Engine compressor stall can be followed by inlet unstart, which could occur through an engine control system failure. Researchers induced this mode of unstart in the following manner:

(1) Set up engine and inlet to run at operating point.
(2) Keep inlet shock positioning control system active to ensure that inlet recovery remains constant until the onset of compressor stall.
(3) Slowly close the VEN to reduce nozzle exit area until compressor stalls. Choose ramp rate that allows corrected engine speed to remain constant until the onset of stall.
(4) Begin transient data recording when high-response differential pressure transducer senses drop in compressor exit static pressure. Record data from -1.0 to 3.0 s (nominal) about the stall event.
(5) Cut fuel flow to the engine.
(6) Allow automatic inlet restart to be performed by override controller.

3.3.3 Test conditions

The nominal test conditions for the data reported herein are: $M_o = 2.20$, $P_o = 11.35$ psia, $T_o = 541$ R, and Re/ft = 2.66×10^6. The tunnel

total pressure and temperature are nominal values since they are averaged over a series of wind tunnel test runs.

4 Experimental Results

The experimental results obtained in this investigation indicate that a propulsion system compressor stall-inlet unstart event adversely affects the surrounding local flow field. The data show the following:

(1) The stall-unstart transient event affects the flow field on a millisecond time scale.
(2) The transient event causes an expanding wave front to propagate outward from the inlet.
(3) The outward wave front propagation is facilitated by the presence of the wing simulator boundary layer.
(4) The flow nearest the wing simulator separates from the surface during the transient event.
(5) A distinct process occurs at the end of the transient event when the affected flow field recovers to free-stream conditions and the wing simulator boundary layer reattaches to the flow surface.

Figure 4 shows the coordinate system used in this investigation. The origins of the coordinate system (0,0,0) are on the wing simulator surface, at the model spanwise centerline, and at the cowl lip axial plane.

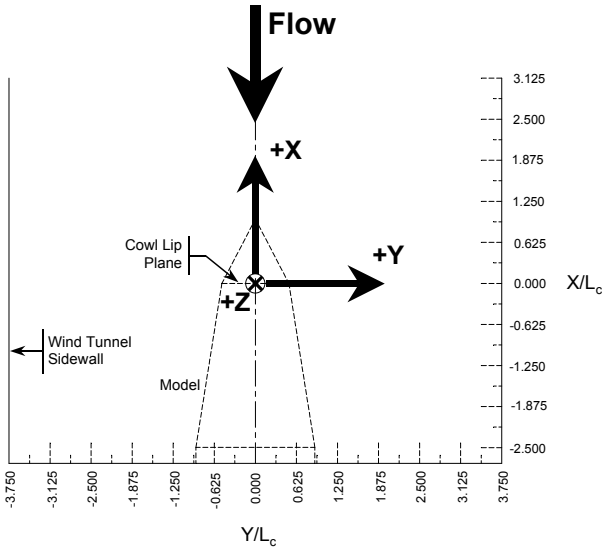

Fig. 4. Coordinate system for experiment (view from above).

4.1 Wing Simulator Static Pressure Measurements

The wing simulator static pressure measurements can be used to track the shock wave – boundary layer interaction caused by the hammershock propagation and give some insight on what is happening in the flow field. In this investigation, an array of axial dynamic static pressure taps (fig. 3) was used to assess the axial extent of the wing simulator surface disturbance propagation. Figure 5 shows the typical wing simulator surface axial static pressure distribution acquired at discrete time steps during an engine compressor stall – inlet unstart event. In all of these plots, the local static pressure is non-dimensionalized by the ambient local static pressure before the stall-unstart event occurs. The indicated time scale is relative to when the stall-unstart event was initially detected on the wing simulator surface, i.e., t = 0 was at the onset of hammershock propagation on wing simulator surface.

Figure 5(a) depicts the undisturbed wing simulator surface axial static pressure distribution just before the hammershock propagates into the flow field. The nondimensional static pressure distribution is relatively uniform at t = -3.33 ms (3.33 ms before stall-unstart event is detected).

For this particular stall-unstart event, the maximum transient static pressure rise due to the hammershock propagation is observed at t = 4 ms (fig. 5(b)) at the near spanwise centerline (Y/L_c = 0.08) and at the axial location X/L_c = 0.625. The maximum observed static pressure ratio was 3.53. By this time, the disturbance has propagated upstream close to X/L_c = 1.875. Note that the steep spanwise static pressure gradient for $X/L_c \le 0.625$ is an artifact of the data reduction; no dynamic static pressure transducers were installed at Y/L_c = ±0.938 spanwise location.

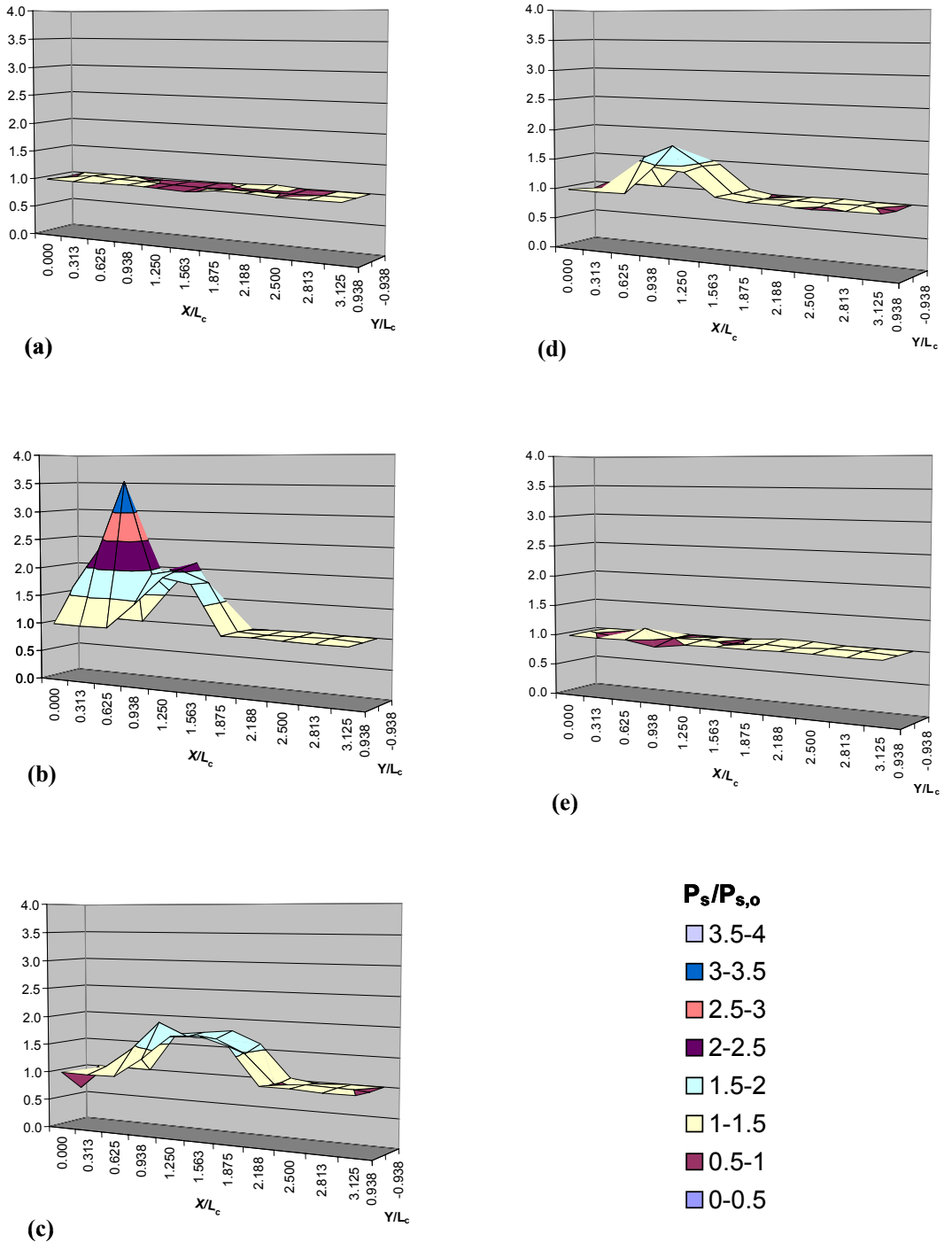

Fig. 5. Typical wing simulator surface axial static pressure distribution during compressor stall-inlet unstart transient event. Free-stream Mach number, M_o, 2.20. (a) Before transient event at t = -3.33 ms. (b) Peak static pressure during transient event at t = 4.00 ms. (c) Maximum axial propagation at t = 9.33 ms. (d) Static pressures recovering from peak axial propagation at t = 14.67 ms. (e) Static Pressures fully recovered from transient event at t = 27.33 ms.

The next event at t = 9.33 ms (fig. 5(c)) depicts the maximum observed forward propagation of the hammershock on the wing simulator surface at X/Lc = 2.188. The static pressure distribution remains relatively constant for 4 ms (t = 8 to 12 ms) at this maximum forward propagation location before beginning to recede. Note the elevated static pressure plateau region that has formed just downstream of the maximum forward propagation point.

Figure 5(d) shows the transient axial static pressure distribution at t = 14.67 ms and captures the hammershock propagation as it recedes from the maximum forward propagation location. At t = 27.33 ms (fig. 5(e)), the static pressure distribution has recovered to the ambient state as evidenced by the relatively uniform static pressure ratio of 1.0. The hammershock propagation phenomenon has completely dissipated.

Note that for the stall-unstart sequence depicted in figure 5, the inlet control system is actively working to restart the inlet as soon as compressor stall is detected. This could lessen the observed maximum forward extent of the disturbance axial propagation when compared with an uncontrolled inlet where no restart attempt is made.

The results depicted herein support the statements at the beginning of this section; namely that the stall-unstart phenomenon causes an expanding wavefront disturbance to propagate upstream on the wing simulator surface as evidenced by the transient static pressure rise, equilibrate with the free stream flow, recede downstream and return to the original free-stream conditions. The observed trends for this particular stall-unstart sequence are typical of what was observed for all stall-unstart transients throughout this investigation.

4.2 Flow-Field Pitot Pressure Measurements

The flow-field pitot pressure measurements acquired during a propulsion system stall-unstart transient event can be used to understand the flow-field physics during the event and assess the extent of the flow field influenced during the event. As mentioned earlier, the pitot pressure instrumentation was mounted on two instrumentation struts placed at discrete axial and spanwise locations relative to the coordinate system origin (fig. 4). For the results presented in this section, the fixed axial and spanwise measurement locations were: $X/L_c = 0.31, 0.94$; and $Y/L_c = \pm 2.15$. This arrangement captures the hammershock propagation flow physics in the axial and Z direction at a constant spanwise distance from the propulsion system centerline.

Figure 6 shows the hammershock propagation in the Z direction captured by the pitot pressure instrumentation during a stall-unstart event. In figure 6(a), the axial measurement station is just forward of the inlet cowl lip at $X/L_c = 0.31$, while the axial measurement station depicted in figure 6(b) is almost one characteristic length upstream of the inlet cowl lip at $X/L_c = 0.94$. It is evident that the hammershock has influenced more of the flow field below the wing simualtor at the axial location nearest the inlet cowl lip plane. At this location, the influence of the hammershock propagation is seen 1.22 characteristic lengths below the wing simulator surface, while the hammershock influences only 0.60 characteristic lengths below the wing simulator at the upstream measurement station. The region influenced by the hammershock in the Z direction progressively decreases as it propagates upstream.

Closer inspection of the individual pitot pressure time histories reveal some interesting trends. At both axial measurement locations, the pitot port closest to the wing simulator first shows the effect of the hammershock propagation followed by each successive pitot port in the Z direction until the outward propagation in the Z direction ceases. This trend indicates that the hammershock disturbance propagates faster along the wing simulator surface and the shape of the hammershock in the flow field has some curvature since each sequential pitot port below the wing simulator is affected at a later time. One possible explanation for this observation is that the hammershock propagation is facilitated by the presence of the subsonic portion of the wing simulator boundary layer.

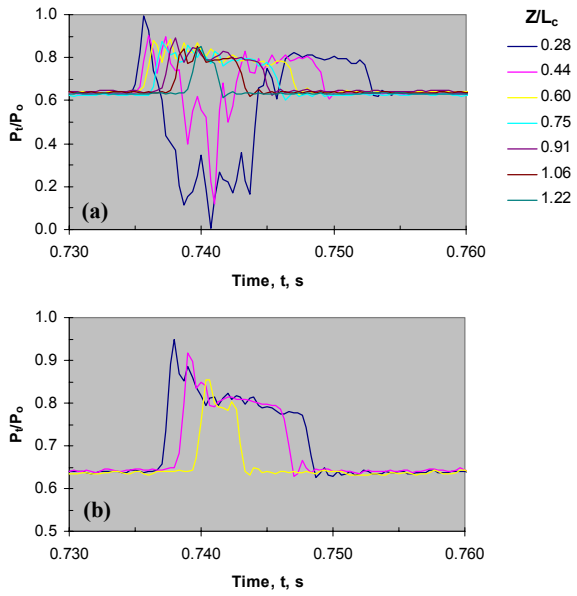

Fig. 6. Pitot pressure time-history profiles perpendicular to wing simulator surface during stall-unstart transient event. Free-stream Mach number, M_o, 2.20; spanwise distance relative to propulsion system centerline, Y/L_c, 2.15. (a) Axial location, X/L_c = 0.31. (b) Axial location, X/L_c = 0.94.

The individual pitot pressure time histories merit some discussion. In all cases, a severe pitot overpressure occurs when the hammershock propagates over the measurement location and exceeds 80 percent of the free-stream total pressure for this particular stall-unstart sequence. This initial overpressure is most severe near the wing simulator surface – here the initial pitot overpressure approaches 100 percent of the free-stream total pressure.

After the initial overpressure, two distinct pitot pressure time histories emerge: (1) A relatively constant overpressure plateau region during the remainder of the hammershock propagation event, and (2) A steep pressure gradient region where the pitot pressure decreases to the local static pressure and then recovers to a relatively constant overpressure plateau during the remainder of the hammershock propagation event. For the stall/unstart event depicted in figure 6, the second pressure distribution occurs only at the axial location nearest the inlet cowl lip and only at the two pitot pressure ports nearest the wing simulator surface. This is a classic indication of flow separation on the wing simulator surface. For this particular stall/unstart event, the time duration of the flow separation is 7 ms. This flow separation phenomenon was observed for all other stall/unstart events in the test program.

The pitot pressure time histories depicted in figure 6(b) best show the nature of the hammershock propagation in the Z direction. The influence of the hammershock is first seen at the measurement location closest to the wing simulator surface, and its outward propagation in the Z-direction shown by the progressive time delay of the onset of pitot overpressure for each successive Z-direction measurement station. At the end of the flow-field transient event, there is distinct evidence that the hammershock disturbance phenomenon begins to propagate inwardly back towards the propulsion system and wing simulator. The last measurement port affected by the hammershock disturbance (Z/L_c = 0.60 in fig. 6(b)) was the first port to recover to the original free-stream pitot pressure. This trend was visible at all measurement stations; that is, all measurement ports recovered in the inverse order in which they were initially affected.

The hammershock disturbance propagation trends also can be seen in the axial direction because of the axial variation in strut position for this stall-unstart event. The pitot pressure data shown in figure 7 show a series of instantaneous Z-direction pitot pressure profiles at both axial measurement locations during the same stall/unstart event depicted in figure 6. Figure 7(a) shows the instantaneous Z-direction pitot profiles 1 ms before (t = -1 ms) the hammershock transient event affects the flow field. The pitot pressure profiles are well behaved and are at the nominal free stream values.

At t = 4 ms, the hammershock disturbance has propagated from the propulsion system to the rearward axial measurement location (X/L_c = 0.31 and Y/L_c = 2.15). This is seen by the severe overpressure shown in figure 7(b) that has affected the flow field 0.8 characteristic lengths below the wing simulator surface. The hammershock has not yet propagated to the upstream measurement location.

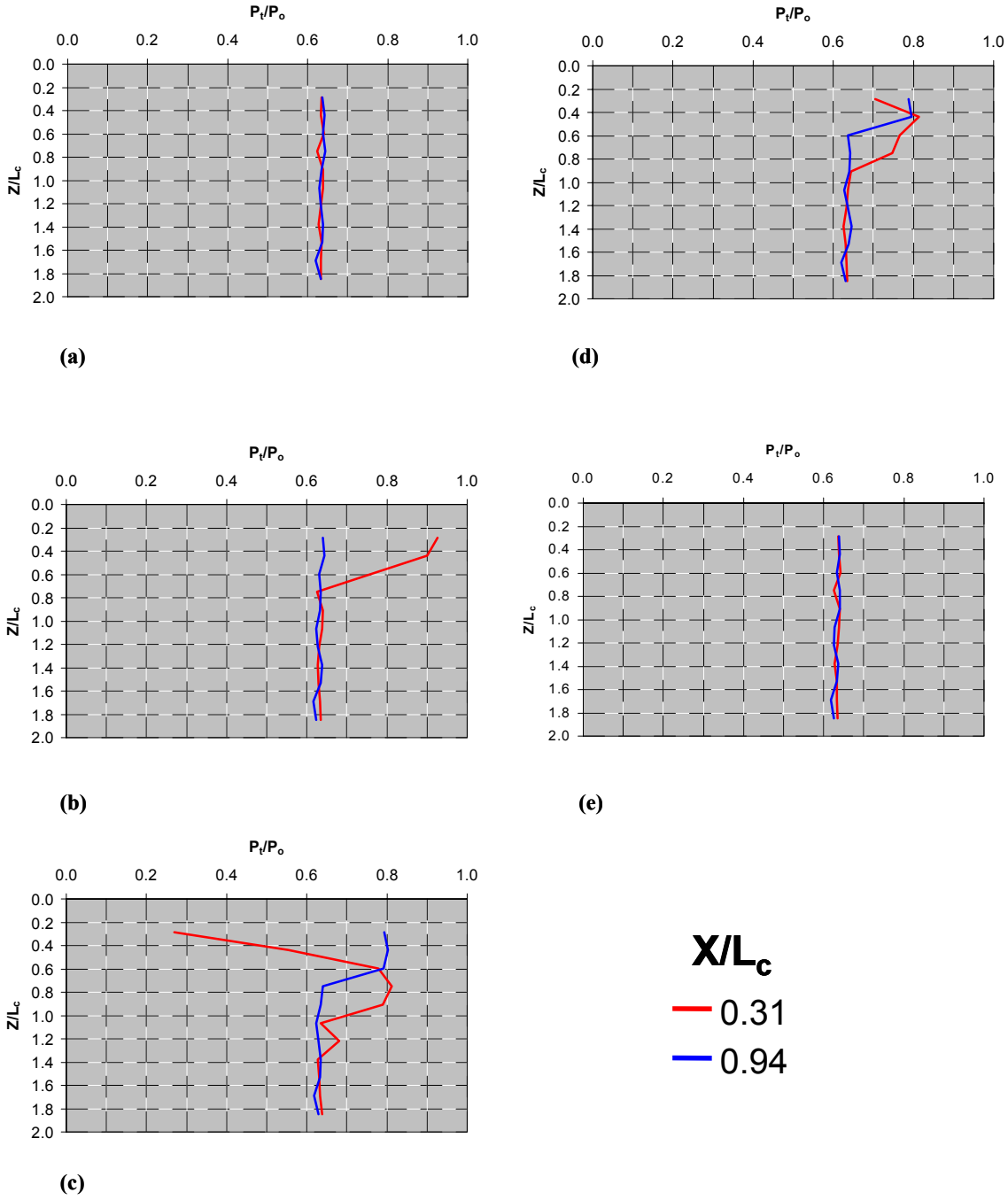

Fig. 7. Instantaneous pitot pressure profiles in the Z-direction perpendicular to the wing simulator surface at two axial stations during compressor stall-inlet unstart transient event. Free-stream Mach number, M_o, 2.20. (a) Before transient event at t = -1 ms. (b) During transient event at t = 4 ms. (c) Maximum extent of influence at t = 9 ms. (d) Pitot pressures as hammershock propagates inward at t = 13 ms. (e) Pitot pressures fully recovered from transient event at t = 22 ms.

At t = 9 ms, the hammershock has propagated past the two axial measurement stations as seen in the Z-direction pitot pressure distributions shown in figure 7(c). At this time step, the hammershock influences the maximum extent of the flow field below the wing simulator – Z/L_c = 1.4 at the rearward measurement plane and Z/L_c = 0.8 at the upstream measurement plane. Again, the extremely low pitot pressure near the wing simulator surface at the rearward measurement plane is evidence of flow separation.

The next two pitot pressure snapshots at t = 13 ms and 22 ms (figs. 7(d) and 7(e)) show the pitot pressure distributions as the hammershock disturbance propagates inward back towards the propulsion system and the flow field finally recovers to free-stream conditions. In figure 7(d), both axial measurement locations are still affected by the hammershock transient, but the Z-direction region of influence has decreased. Figure 7(e) shows the full flow field recovery to free-stream conditions after the hammershock transient has completely dissipated.

The pitot pressure data presented herein substantiate the statements made at the beginning of section four; namely that the stall-unstart phenomenon causes an expanding wavefront disturbance to propagate upstream through the flow field, come to equilibrium with the free-stream flow, recede downstream and return to the original free-stream conditions. The observed trends in the flow field pitot pressure behavior for this particular stall-unstart sequence are typical of what was observed for all stall-unstart transients throughout this investigation.

5 Concluding Remarks

A wind tunnel test was conducted to acquire flow-field data during a supersonic propulsion system compressor stall and inlet unstart sequence. The propulsion system consisted of a mixed compression, two-dimensional bifurcated inlet coupled to a General Electric J85-13 turbojet engine. The propulsion system was mounted below a large flat plate that simulated an underwing propulsion pod installation. Flow-field pitot pressure and wing simulator surface static pressure data were acquired during multiple stall-unstart sequences at a free-stream Mach number of 2.20.

The results indicate that an engine compressor stall followed by a mixed-compression inlet unstart causes a three-dimensional hammershock disturbance to propagate from the propulsion system into the surrounding flow field. The three-dimensional disturbance propagates outward until it equilibrates with the free-stream flow field. After the equilibration process, the disturbance appears to collapse and all flow field properties return to the original free-stream conditions. The whole process occurs within approximately 30 ms for the stall-unstart sequences analyzed in this paper.

References

[1] Soeder, R.H. User Manual for NASA Lewis 10 by 10 Foot Supersonic Wind Tunnel. Revised, NASA TM-105626, 1995.

[2] Porro, A.R. Pressure Probe Designs for Dynamic Pressure Measurements in a Supersonic Flow Field. *ICIASF 2001 Record*, Cleveland, OH, paper 13.1, pp 417-426, 2001.